Int. J. Electrochem. Sci., 14 **(2019)** 11391 – 11405, doi: 10.20964/2019.12.07

International Journal of
ELECTROCHEMICAL
SCIENCE
www.electrochemsci.org

Effects of Zn Doping Amount on the Electrochemical Properties of $LiNi_{0.5}Mn_{1.5}O_4$ Lithium-Ion Cathode Materials

Hongyan Sun [1,2], *Xin Kong* [1,2], *Shaoping Feng* [1,2], *Guiyang Liu* [1,2,*]

[1] Department of Chemistry, College of Science, Honghe University, Mengzi, 661199, Yunnan, China
[2] Local Characteristic Resource Utilization and New Materials Key Laboratory of Universities in Yunnan, Honghe University, Mengzi 661199, Yunnan, China.
[*]E-mail: liuguiyang@tsinghua.org.cn

Received: 27 June 2019 / *Accepted:* 2 September 2019 / *Published:* 29 October 2019

The effects of Zn doping for Mn site on the electrochemical properties of $LiNi_{0.5}Mn_{1.5-x}Zn_xO_4$ (x=0, 0.01, 0.03, 0.05, 0.08, 0.10) have been systematically investigated. The $LiNi_{0.5}Mn_{1.5-x}Zn_xO_4$ samples, which were synthesized by a modified low temperature solution combustion synthesis method, were characterized by X-ray diffraction(XRD), infrared spectroscopy(FT-IR), scanning electron microscopy(SEM), galvanostatic charge-discharge testing, cyclic voltammetry(CV) and electrochemical impedance spectroscopy(EIS). All samples have perfect cubic spinel structures with a combination of ordered and disordered space groups. The microstructure is almost not affected by the amount of Zn doping obtained from the SEM results. The electrochemical performances are obviously improved by Zn doping, which are shown from cycle stability, rate capability and high temperature cycling performance. The cycle performance is promoted with the increasing of Zn doping content both at 25 ºC and at elevated temperature of 55 ºC. The first charge-discharge efficiency and rate capability first increase and then decrease with the increase of Zn doping content, which is best when the Zn doping content is 0.05. Meanwhile, the impedance of products significantly decreases after Zn doping.

Keywords: Electrochemical performance, $LiNi_{0.5}Mn_{1.5}O_4$, lithium-ion batteries, Mn site, Zn doping

1. INTRODUCTION

Recently, lithium-ion batteries(LIBs) have been considered as the promising power sources for electric vehicles (EVs) and hybrid electric vehicles (HEVs) [1, 2]. In fact, cathode materials play a vital role in determination of electrochemical performance of the LIBs. At the same time, the cathode material is an important component of the LIBs, accounts for about 40% of the cost of batteries. Many different kinds of LIBs cathode materials have been explored in the past two decades. Among these cathode materials, the $LiNi_{0.5}Mn_{1.5}O_4$(LNMO) spinel delivers high energy density, high operating

voltage, high rate capability, etc.[3-5], making it a promising LIBs' positive material in practical use. However, numerous works report that the LNMO usually shows obvious capacity degradation at high temperature(≈55 ^{o}C)[6]. So researchers have made a lot of efforts to overcome this problem, such as by modifying synthetic route, by controlling special morphologies, by surface coating, and so on. According to related reports, the performance of LNMO cathode materials can be effectively improved by doping cations or anions. The doping elements mainly including Na[6], Zn, Cu[7], Mg[8], Fe[9], Al[8], Cr[9], Zr[10], V[11], W[12], F[13] and S[14], etc., which can indeed enhance the electrochemical performance of the LNMO materials.

Zn-doping can indeed increase the cyclic stability of the LNMO which first reported by Manthiram et al.[15]. A series of $LiZn_xNi_{0.5-x}Mn_{1.5}O_4$((x=0, 0.02, 0.04, 0.08, 0.25 and 0.5) spinel materials were successfully synthesized using the sol-gel method by Yang et al. [16]. The results showed that the $LiZn_{0.08}Ni_{0.42}Mn_{1.5}O_4$ delivered improved cycle-life and C-rate performance both at home temperature and at elevated temperature, attributing to forming a thick interphase film between the positive electrode and the electrolyte. Encouraged by these results, our group have successfully synthesized the $LiNi_{0.5}Mn_{1.45}Zn_{0.05}O_4$ with a novel solution combustion synthesis method[17]. The result showed that it indeed could improve the cyclic stability and the rate capability significantly. Here what needs to be emphasized is that the substitution of Zn is not on Ni site but on Mn site in our study. For further systematically study the effects of Zn doping amount on the electrochemical properties of LNMO, $LiNi_{0.5}Mn_{1.5-x}Zn_xO_4$ (x=0, 0.01, 0.03, 0.05, 0.08, 0.10) spinel samples were prepared in the paper.

2. EXPERIMENTAL

2.1 Synthesis

The modified low temperature solution combustion synthesis method were used to synthesize the $LiNi_{0.5}Mn_{1.5-x}Zn_xO_4$ (x=0, 0.01, 0.03, 0.05, 0.08, 0.10) spinel samples. The lithium nitrate, lithium acetate, nickel nitrate, nickel acetate, manganese nitrate, manganese acetate and zinc acetate were working as raw materials and the molar ratio of nitrate and acetate for all metals was 1:1. The synthesis process of materials was described in detail in our other studies[7, 17].

2.2 Characterization

The Powder X-ray diffraction (XRD, PANalytical X'pert pro, Cu-Ká radiation) and the Fourier transformed infrared spectroscopy(FTIR, PerkinElmer, with KBr pellets) were employed to characterize the phase structure and crystal structure of the samples. The field emission scanning electron microscopy(SEM, FEI Quanta FEG 250) was used to observe the morphologies of products.

The electrochemical properties of each sample were measured using a CR2025-type coin cell, which composed of cathode, lithium anode, Celgard polyethylene separator, and $LiPF_6$ in 1:1 ethylene carbonate(EC) and dimethyl carbonate(DEC) as electrolyte. The detailed preparation flow of cathode

electrodes and coin cells were described in our previous research[17]. The cells were galvanostatically cycled on a muti-channel battery cycler(LANHE CT2001A instrument, Wuhan, China) in the voltage window for 3.5 to 5.0V. The cells were also cycled at 55 ºC by putting them in an oven. Cyclic voltammogram(CV) of the cells was measured on a CHI 660 electrochemical workstation from 3.5-5.0V at different scan rates from 0.1 to 0.5mV/s. Electrochemical impedance spectroscopy (EIS) is collected at charging state of fully lithiation with an ac amplitude voltage of 5mV in the frequency range of 100 kHz to 0.1 Hz, using the CHI 660 electrochemical workstation.

3. RESULTS AND DISCUSSION

3.1 Structure

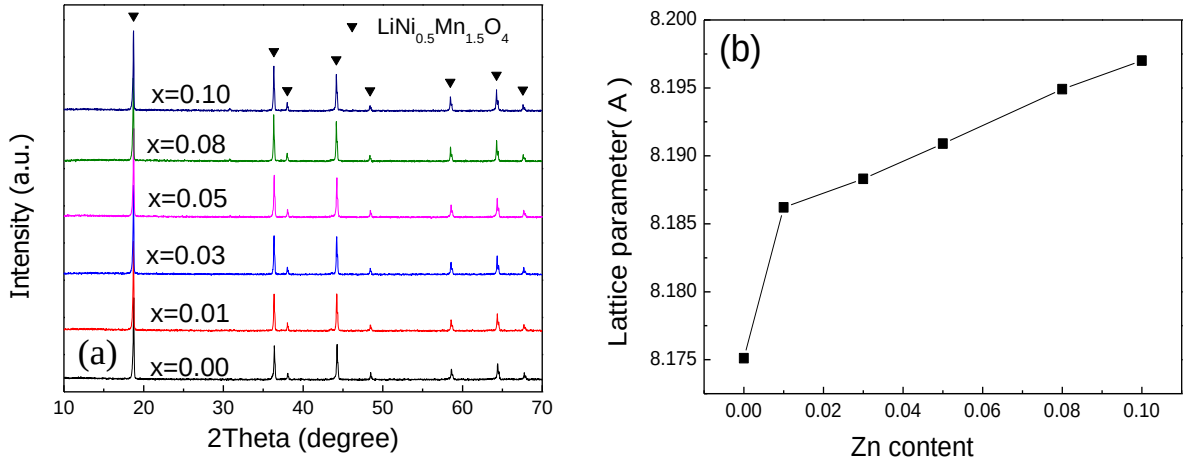

Figure 1. (a) XRD patterns and (b) lattice parameters of $LiNi_{0.5}Mn_{1.5-x}Zn_xO_4$ (x=0, 0.01, 0.03, 0.05, 0.08, 0.10)

The X-ray diffraction patterns of the spinel powders are shown in Fig. 1(a). All of the diffraction peaks are assigned to the spinel compound $LiNi_{0.5}Mn_{1.5}O_4$ and no impurity peak is found in the products. The lattice parameter obviously increases after Zn doping, which is shown in Fig. 1(b). To our knowledge, the ionic radius of Zn is 0.074nm, which is larger than those of Mn^{3+}(0.058nm) and Mn^{4+} (0.053nm)[18], suggesting that the Zn element has successfully substituted some Mn element. In the meantime, it is found that the crystal lattice parameter increases with the increase of Zn doping content in a similar linear relationship.

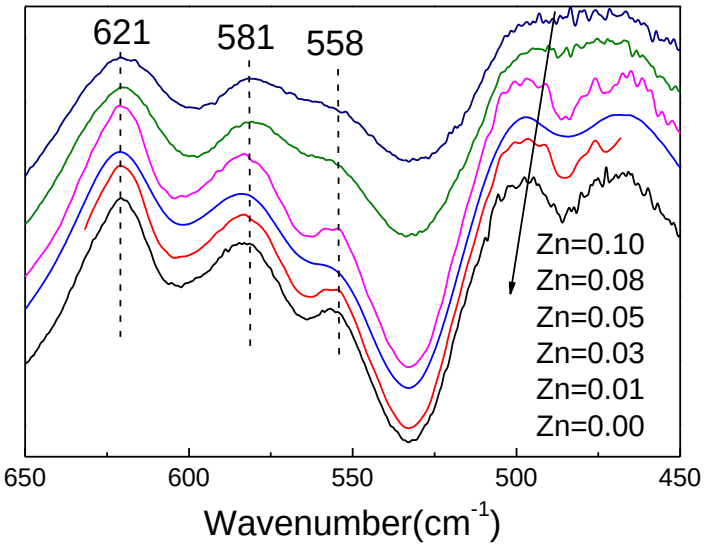

Figure 2. FT-IR spectra of $LiNi_{0.5}Mn_{1.5-x}Zn_xO_4$ (x=0, 0.01, 0.03, 0.05, 0.08, 0.10)

FT-IR spectroscopy has been proved to be an effective technique in identification of the $P4_332$ and Fd-3m spinel of the LNMO[19]. As shown in Fig. 2, the obvious bands at 558cm^{-1}, which is the characteristic peak reported by Wang[20], show the existence of ordered phase in the products. Meanwhile, all samples show lower band intensity at 581cm^{-1} than that at 621cm^{-1}, suggesting that the products have disorder space group Fd-3m[21]. Therefore, the conclusion can be drawn that all the samples contain two phases of ordered and disordered. In fact, Patoux et al. have also reported the same phenomenon in their study[22]. According to Kim and Zheng[23, 24], the LNMO with some disordered crystallographic structure usually has higher electronic conductivity, because of the existence of some Mn^{3+}.

3.2 Morphology

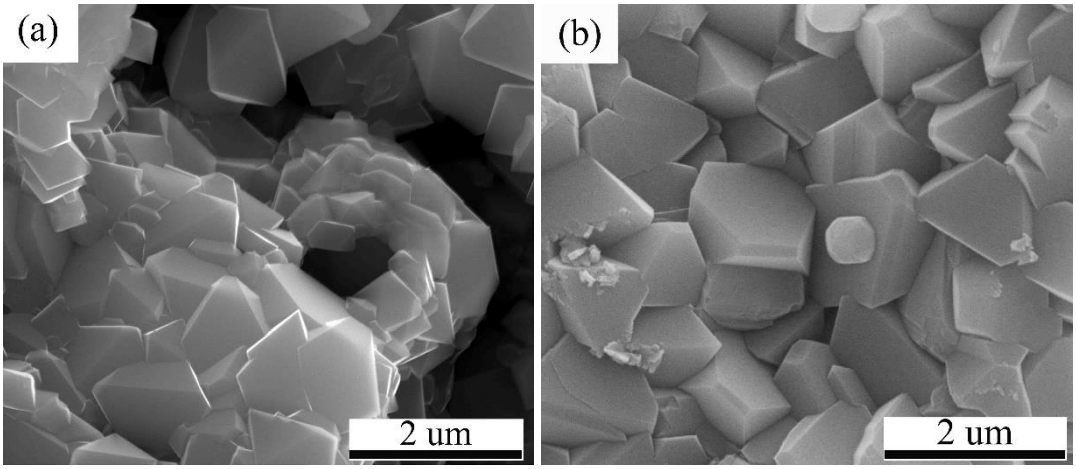

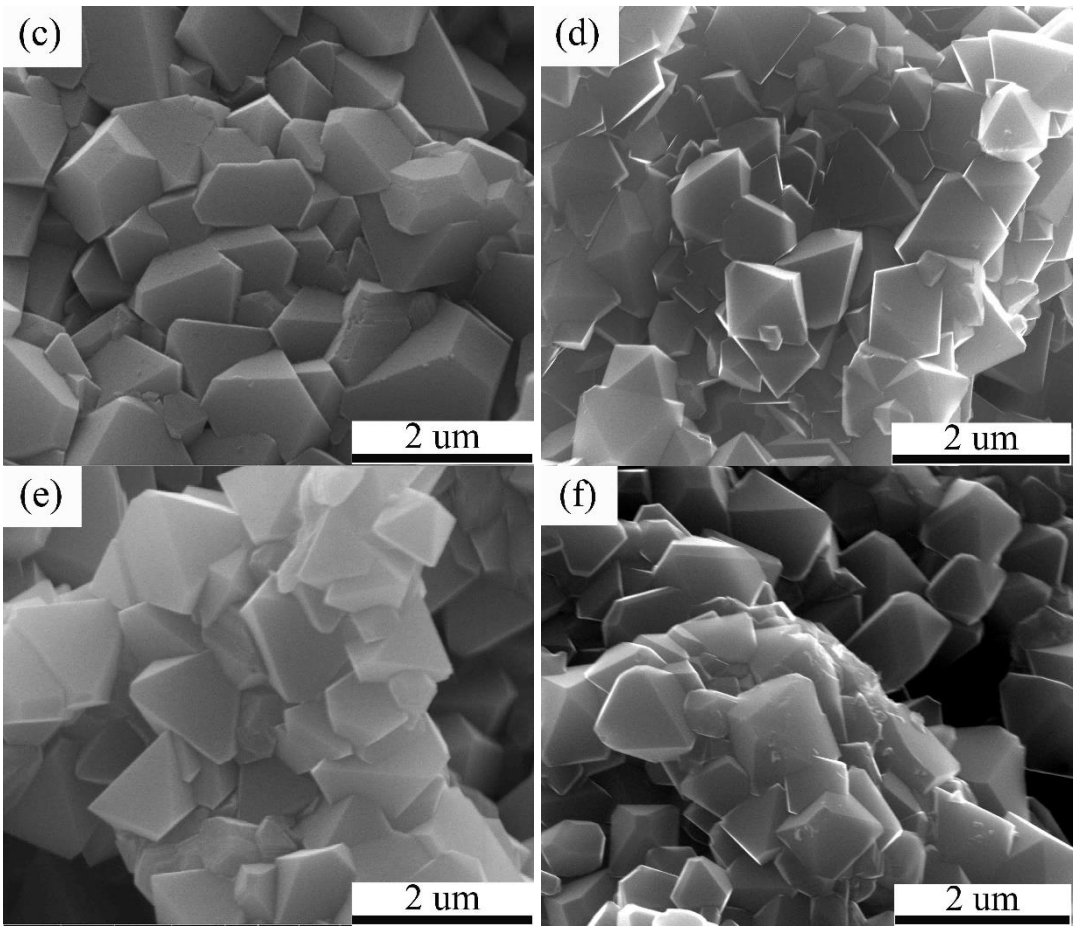

Figure 3. SEM images of $LiNi_{0.5}Mn_{1.5-x}Zn_xO_4$: (a) x=0.00, (b) x=0.01, (c) x=0.03,(d) x=0.05, (e) x=0.08 and (f) x=0.10

Fig. 3 shows the SEM images of the products. The micro morphologies of all samples are similar. It is obvious that the microstructure of samples is not affected by Zn doping. In the meantime, Fig. 3 illustrates that the products exhibit perfect octahedral spinel structure with homogeneous particles.

3.3 Electrochemical performance

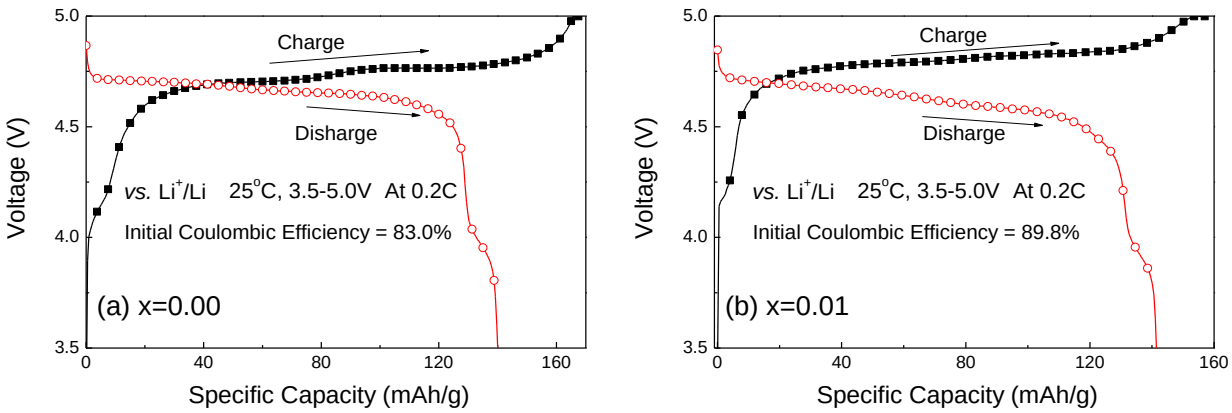

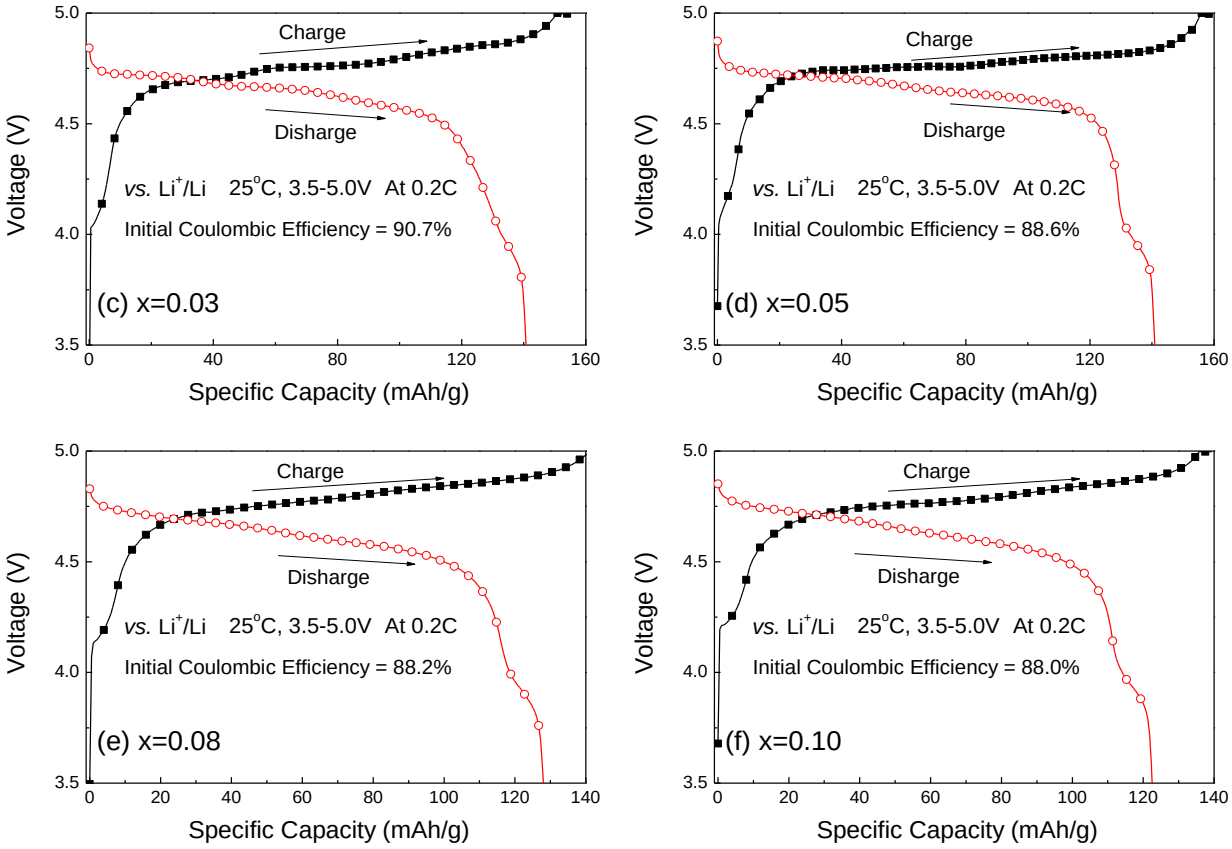

Figure 4. Initial charge/discharge curves of $LiNi_{0.5}Mn_{1.5-x}Zn_xO_4$: (a) x=0.00, (b) x=0.01, (c) x=0.03, (d) x=0.05, (e) x=0.08 and (f) x=0.10 between the 3.5 and 5V regions(vs. Li^+/Li) at 0.2C rate at 25ºC

Fig. 4 gives the initial consecutive charge and discharge profiles for the $LiNi_{0.5}Mn_{1.5-x}Zn_xO_4$ (x=0, 0.01, 0.03, 0.05, 0.08, 0.10) samples. All charge and discharge curves exhibit two potential plateaus at around 4.7V and 4.0V, which corresponding to the reduction/oxidation peaks of Ni^{2+}/Ni^{4+} and Mn^{3+}/ Mn^{4+} redox, respectively. This conclusion is in consistent with the FT-IR results above. Their initial discharge specific capacities are 140, 141.4, 140.7, 140.9, 128 and 122.5mAh/g, respectively. Obviously, the initial discharge capacity is higher than $LiNi_{0.5}Mn_{1.5-x}Cu_xO_4$(x=0, 0.03, 0.05, 0.10, 0.15) samples in our other research [7]. As shown in Fig. 4, the specific capacities decrease gradually with the increasing of Zn doping amount, especially when the Zn doping amount is more than 0.05. The initial coulombic efficiency of $LiNi_{0.5}Mn_{1.5-x}Zn_xO_4$ (x=0, 0.01, 0.03, 0.05, 0.08, 0.10) samples are 83.0%, 89.8%, 90.7%, 88.6%, 88.2% and 88.0%, respectively. The initial charge-discharge efficiency first increases and then decreases with the increasing of Zn doping amount. The initial coulombic efficiency reaches the maximum value of 90.7% when the doping amount of Zn is 0.03.

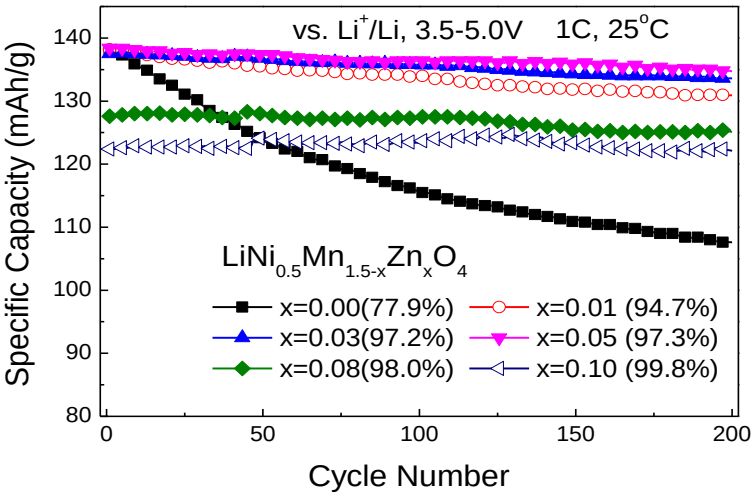

Figure 5. Cycling performance of $LiNi_{0.5}Mn_{1.5-x}Zn_xO_4$ (x=0, 0.01, 0.03, 0.05, 0.08, 0.10) in the potential range of 3.5-5V(vs. Li^+/Li)at 1C rate at 25°C

The cycling performance profiles of the products at 1C rate and 25°C are given in Fig. 5. It is observed that Zn-doping can significantly improve the cycling performances of the LNMO spinel. The cycling performances are gradually promoted with the increasing of Zn doping amount. The capacity has almost no attenuation after 200 cycles when the Zn doping content is 0.10. The cycle stability of the products of $LiNi_{0.5}Mn_{1.5-x}Zn_xO_4$ (x=0, 0.01, 0.03, 0.05, 0.08, 0.10) are better, comparing with the $LiZn_xNi_{0.5-x}Mn_{1.5}O_4$ (x=0, 0.02, 0.04, 0.08, 0.25, 0.5) materials prepared by Yang et al.[16]. The results reveal that doped zinc on Mn site in LNMO is more favorable for the reversible intercalation and deintercalation of Li^+ than that of on Ni site.

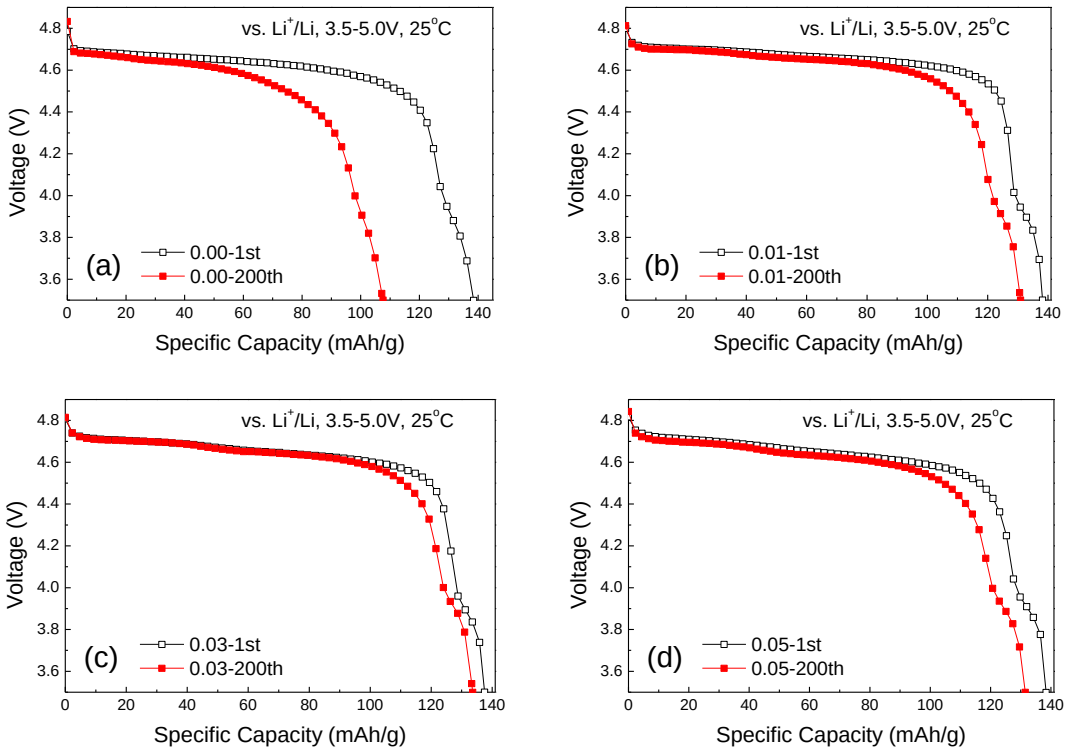

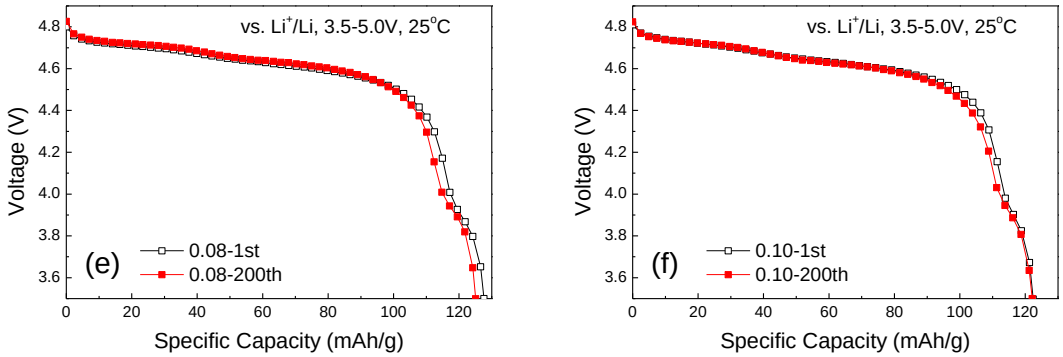

Figure 6. The discharge curves of the first and the 200th cycles at 1C and 25ºC of $LiNi_{0.5}Mn_{1.5-x}Zn_xO_4$ (a) x=0.00, (b) x=0.01, (c) x=0.03, (d) x=0.05, (e) x=0.08 and (f) x=0.10

In Fig. 6, the discharge curves of the first and the 200th cycles at 1C and 25ºC of the products (a) Zn=0.00, (b) Zn=0.01, (c) Zn=0.03, (d) Zn=0.05, (e) Zn=0.08 and (f) Zn=0.10 are shown. From Fig. 6, it can be seen that the stability of voltage platform increases with the increase of Zn doping content under cyclic loading. There was almost no change in the voltage platform after 200 cycles when the Zn doping amount is more than 0.03, indicating that the products have good cyclic stability.

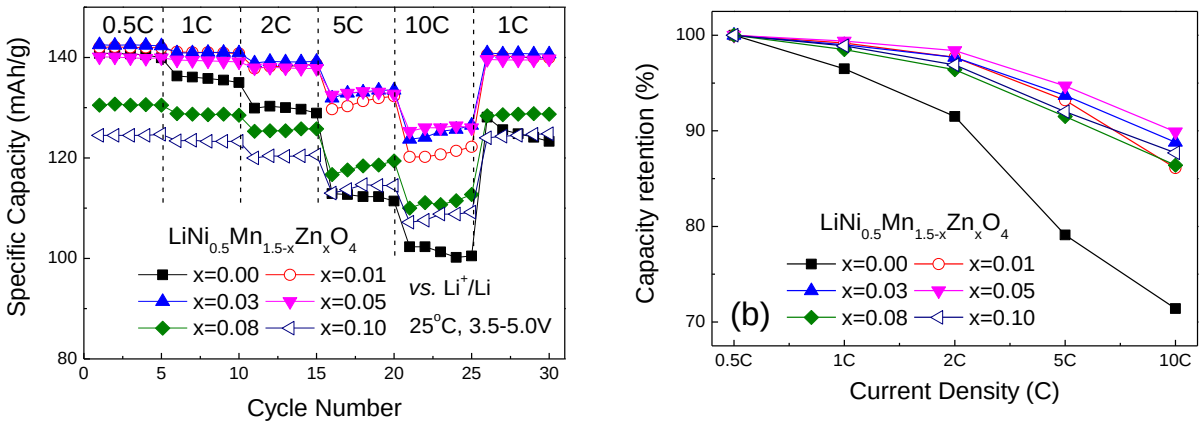

Figure 7. Rate capabilities and capacity retentions of $LiNi_{0.5}Mn_{1.5-x}Zn_xO_4$ (x=0, 0.01, 0.03, 0.05, 0.08, 0.10) at different rates ranged from 0.5 to 10C at 25ºC

Fig. 7 depicts the rate capabilities and capacity retentions of the products at different rates. As shown in Fig. 7, after Zn doping, the rate capability of all products gets a significant enhancement. And the best rate capability is obtained when the Zn doping content is 0.03 and 0.05. Meanwhile, the specific capacity of $LiNi_{0.5}Mn_{1.45}Zn_{0.05}O_4$ is still high to 126mAh/g at high rate of 10C, which is higher than the Co_3O_4-coated LNMO materials prepared by Guo et al.[25].

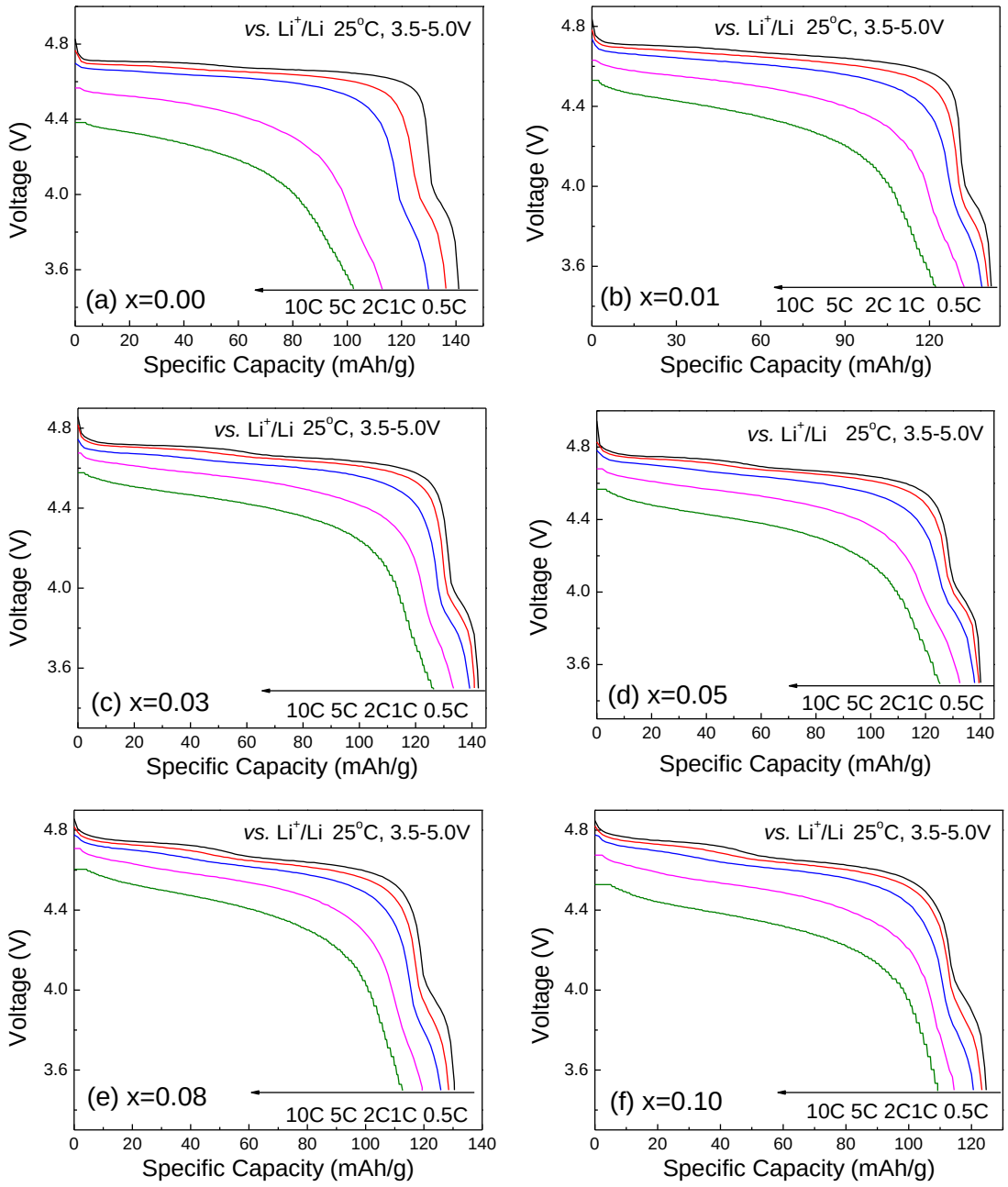

Figure 8. The discharge curves at different C-rates of $LiNi_{0.5}Mn_{1.5-x}Zn_xO_4$ (x=0, 0.01, 0.03, 0.05, 0.08, 0.10) at 25°C in the potential range of 3.5-5V(vs. Li^+/Li)

The discharge voltage profiles of the $LiNi_{0.5}Mn_{1.5-x}Zn_xO_4$ (x=0, 0.01, 0.03, 0.05, 0.08, 0.10) samples at C-rates of 0.5-10C and room temperature over a potential window of 3.5-5.0V are demonstrated in Fig. 8. Obviously, the voltage platform is significantly promoted by Zn doping.

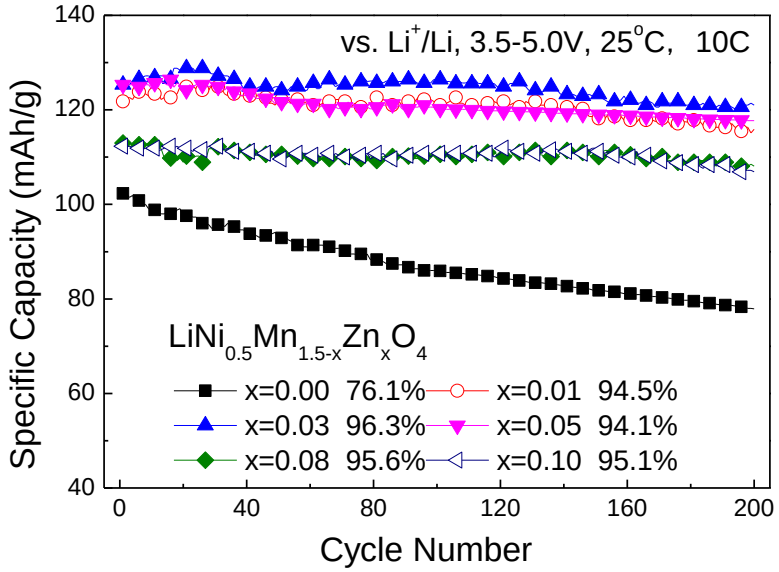

Figure 9. The cycling performance of $LiNi_{0.5}Mn_{1.5-x}Zn_xO_4$ (x=0, 0.01, 0.03, 0.05, 0.08, 0.10) at 10 C rate and 25°C in the potential range of 3.5-5V(vs. Li^+/Li)

The cycling performance of the products at a high rate of 10 C and 25°C is shown in Fig. 9. The capacity retentions of $LiNi_{0.5}Mn_{1.5-x}Zn_xO_4$ (x=0, 0.01, 0.03, 0.05, 0.08, 0.10) samples are 76.1%, 94.5%, 96.3%, 94.1%, 95.6% and 95.1% after 200 cycles, respectively. Clearly, the cycling stability of the products at a high rate of 10C is significantly improved after Zn doping.

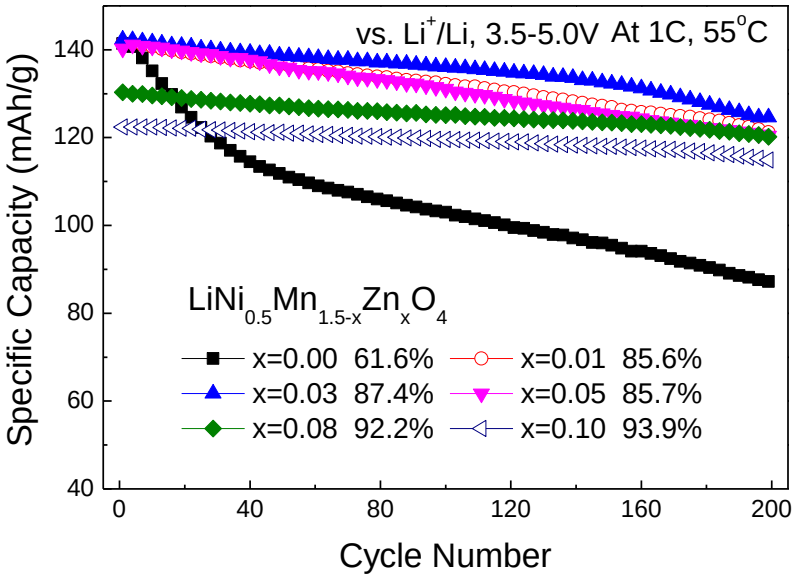

Figure 10. The cycling performances of $LiNi_{0.5}Mn_{1.5-x}Zn_xO_4$ (x=0, 0.01, 0.03, 0.05, 0.08, 0.10) at 1C rate and 55 °C in the potential range of 3.5-5V(vs. Li^+/Li)

Fig. 10 presents the typical cyclic performance of products at 1C rate between 3.5 and 5V and 55 °C. The capacity retentions are 61.6%, 85.6%, 87.4%, 85.7%, 92.2% and 93.9% for

$LiNi_{0.5}Mn_{1.5-x}Zn_xO_4$ (x=0, 0.01, 0.03, 0.05, 0.08, 0.10) samples after 200 cycles. Obviously, the cyclic stability of samples at elevated temperature is greatly improved after Zn doping. The capacity retention rate of $LiNi_{0.5}Mn_{1.40}Zn_{0.10}O_4$ is still 93.9% after 200 cycles at 55ºC, which is better than some Refs [26, 27]. It is likely may be that Zn-doping on Mn site can make the samples have more stable structure.

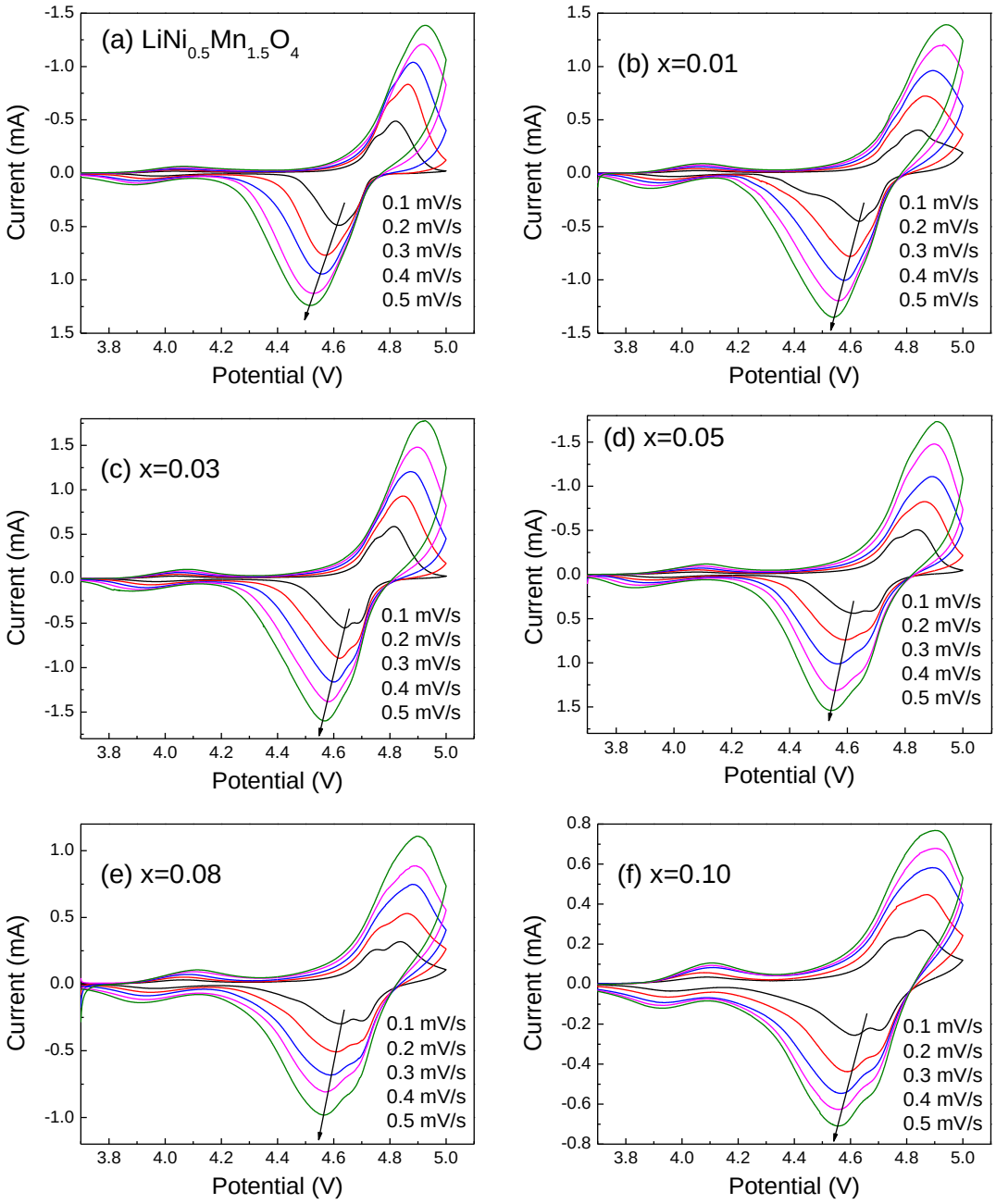

Figure 11. The CV curves of $LiNi_{0.5}Mn_{1.5-x}Zn_xO_4$ (x=0, 0.01, 0.03, 0.05, 0.08, 0.10) at different scanning rates ranged from 0.1 to 0.5mV/s at 25 ºC in the potential range of 3.5-5V(vs. Li^+/Li)

Fig. 11 shows the cyclic voltammetry (CV) curves of the products recorded from 0.1mV/s to 0.5mV/s scan rates. Two pairs of redox peaks can be clearly observed in the CVs. The strong peak at

around 4.7V responds to $Ni^{2+/4+}$ redox couple no splitting two separate peaks, which is generally accepted in $P4_332$ ordered space group, while the minor peak at around 4.0V corresponds to $Mn^{4+/3+}$ redox couple due to the oxygen deficiencies in the disordered spinel. The results indicate that the products have a mixture structure of ordered and disordered, consistent with the FT-IR analysis.

In order to study the diffusion kinetics and the diffusion coefficients of Li^+, the linear relationship between the peak current (i_p) and the square root of the scan rates ($v^{1/2}$) of $LiNi_{0.5}Mn_{1.5-x}Zn_xO_4$ (x=0, 0.01, 0.03, 0.05, 0.08, 0.10) samples is plotted in Fig. 12 with the formula as follows[28]:

$$i_p = 2.69\times10^5 n^{3/2} A C_{Li} D_{Li}^{1/2} v^{1/2}$$

Here, n=1, A=2cm^2, C_{Li}= 0.02378 mol/cm^3.

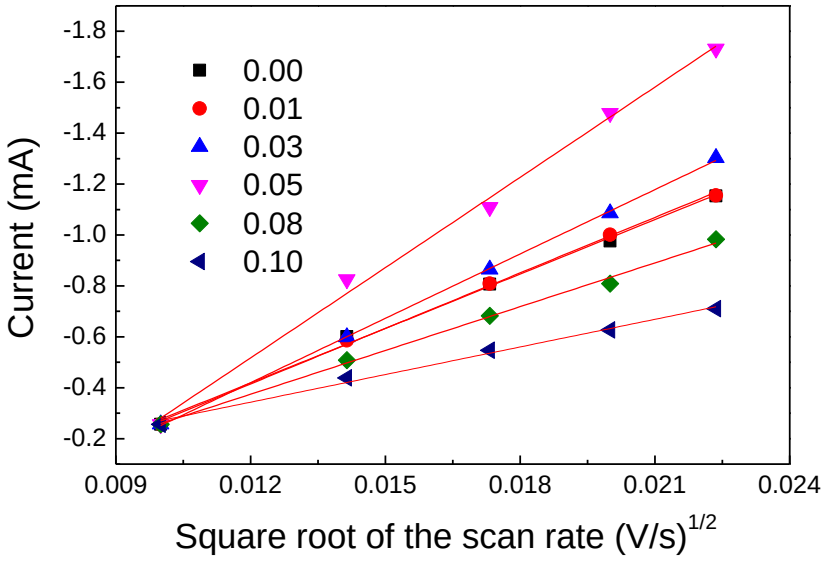

Figure 12. The i_p vs. the square root of the scan rates ($v^{1/2}$) of $LiNi_{0.5}Mn_{1.5-x}Zn_xO_4$ (x=0, 0.01, 0.03, 0.05, 0.08, 0.10)

As shown in Fig. 12, the slope of the $LiNi_{0.5}Mn_{1.5-x}Zn_xO_4$ (x=0, 0.01, 0.03, 0.05, 0.08, 0.10) samples are -71.32,-72.68, -84.26, -118.21, -57.3 and -36.1, respectively. Meanwhile, the chemical diffusion coefficient of Li^+(D_{Li}) of the as-prepared samples are calculated as shown in Table 1. Obviously, the slope first increases and then decreases with the increasing of Zn doping amount. The slope reaches the maximum value when the Zn doping amount is 0.05, and at this time the Li ion conductivity is 8.52E-11. Maybe it is because that the Li-ion diffusion path will be blocked by the excess doped Zn ions and resulting in the decreasing of D_{Li}, which was also reported in our other study of Cu doped $LiNi_{0.5}Mn_{1.5-x}Cu_xO_4$ samples [7].

Table 1. The D_{Li} of prepared $LiNi_{0.5}Mn_{1.5-x}Zn_xO_4$(x=0, 0.01, 0.03, 0.05, 0.08, 0.10)

$LiNi_{0.5}Mn_{1.5-x}Zn_xO_4$	$D_{Li}/(cm^2 \cdot s^{-1})$
x=0.00	3.10E-11
x=0.01	3.22E-11
x=0.03	4.33E-11
x=0.05	8.52E-11
x=0.08	2.00E-11
x=0.10	7.95E-12

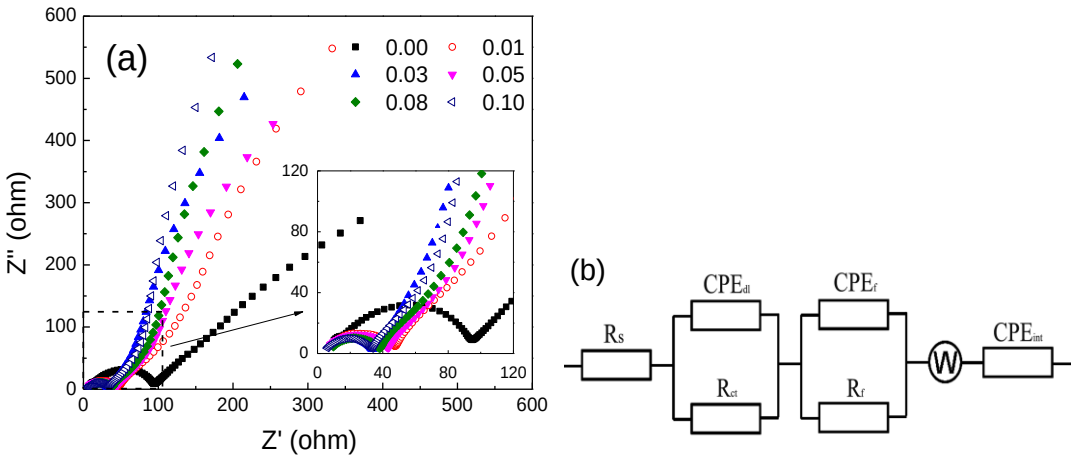

Figure 13. The electrochemical impedance spectral(EIS) and a possible equivalent circuit of $LiNi_{0.5}Mn_{1.5-x}Zn_xO_4$ (x=0, 0.01, 0.03, 0.05, 0.08, 0.10) in the frequency range from 0.1Hz to 100kHz.

To further understand the reasons for the excellent electrochemical properties of LNMO-Zn samples, the electrochemical impedance spectroscopy (EIS) studies are carried out in the frequency range from 0.1Hz to 100kHz. All the samples are cycled 3 cycles and then charged to 5.0V. The EIS spectra are shown in Fig. 13(a). And the possible equivalent circuit for the samples is also proposed in Fig. 13(b). All the EIS spectra have similar profiles which are consist of a semi-circle at high-to-middle frequency region is assigned to the charge transfer resistance (R_{ct}+ R_f) and an inclined line in the low frequency region is resulted from the lithium ion diffusion resistance in the spinel(W). And the R_s is attributing to the ohimic resistance of the electrolyte. As shown, the R_{ct} and R_f values of Zn-doping samples are much smaller than the LNMO spinel, implying that the Zn-doping samples have much lower electrochemical polarization which can lead to higher rate capability, which is in good consistent with the above C-rate capacity results.

4. CONCLUSIONS

In summary, the Zn-doped $LiNi_{0.5}Mn_{1.5-x}Zn_xO_4$ (x=0, 0.01, 0.03, 0.05, 0.08, 0.10) are synthesized via the modified low temperature solution combustion synthesis method. The obtained powders have a combination structure of ordered and disordered space group and exhibit perfect cubic spinel structures. The microstructure of samples will not affected by Zn doping. The cyclic stability of Zn-doping samples at 55ºC and room temperature have significantly enhanced at 1C rate comparing with the LNMO spinel. The capacity has almost no attenuation after 200 cycles when the Zn doping amount is 0.10 at room temperature. Even at 55℃, the capacity retention of $LiNi_{0.5}Mn_{1.40}Zn_{0.10}O_4$ is high to 93.9% after 200 cycles. Meanwhile, the Zn-doping samples show better rate capability and improved cyclic performance at high rate of 10C at room temperature. The $LiNi_{0.5}Mn_{1.47}Zn_{0.03}O_4$ sample can keep a capacity retention of 96.3% at 10C after 200 cycles.

ACKNOWLEDGEMENT
The authors thank the financial supports from the National Natural Science Foundation of China(No. 51362012, No. 51662007 and U1602273), the Yunnan Local Colleges (part) Applied Basic Projects Joint Special Foundation (2017FH001-120) and the Yunnan Applied Basic Research Project (No.2017FD157).

References

1. S. Patoux, L. Sannier, H, Lignier, Y. Reynier, C. Bourbon, S. Jouanneau, F.L. Cras and S. Martinet, *Electrochim. Acta*, 53 (2008) 4137.
2. T.F. Yi, J. Mei and Y.R. Zhu, *J. Power Sources*, 316 (2016) 85.
3. G.Q. Liu, J.Y. Zhang, X.H. Zhang, Y.L. Du, K. Zhang, G.C. Li, H. Yu, C.W. Li, Z.Y. Li, Q. Sun and L. Wen, *J. Alloys Compd.*, 725 (2017) 580.
4. W. Wu, J.L. Guo, X. Qin, C.B Bi, J.F Wang, L. Wang and G.C. Liang, *J. Alloys Compd.*, 721 (2017) 721.
5. Y. Luo, H.Y. Li, T.L. Lu, Y.X. Zhang, S.S. Mao, Z. Liu, W. Wen, J.Y. Xie and L.Q. Yan, *Electrochim. Acta*, 238 (2017) 237.
6. J. Wang, W.Q. Lin, B.H Wu and J.B Zhao, *Electrochim. Acta*, 145 (2014) 245.
7. H.Y. Sun, X. Kong, B.S. Wang, T.B. Luo and G.Y. Liu, *Ceram. Int*., 44 (2018) 4603.
8. G.Y. Liu, H.Y. Sun, X. Kong, Y.N. Li and B.S. Wang, *Int. J. Electrochem. Sci*., 10 (2015) 6651.
9. D.W. Shin, C.A. Bridges, A. Huq, M.P. Paranthaman and A. Manthiram, *Chem. Mater.*, 24 (2012) 3720.
10. S.P. Feng, X. Kong, H.Y. Sun, B.S. Wang, T.B. Luo and G.Y. Liu, *J. Alloys Compd.*, 749 (2018) 1009.
11. M.C. Kim，K.W. Nam，E. Hu, X.Q. Yang, H.Kim, K. Kang, V. Aravindan, W.S. Kim and Y.S. Lee, *ChemSusChem* 7 (2014) 829.
12. S.J. R. Prabakar, S.C.Han, S.P. Singh, D.K.Lee, K.S.Sohn and M. Pyo, *J. Power Sources*, 209 (2012) 57.
13. Y.H. Xu, S.X. Zhao,Y.F. Deng, H. Deng and C.W. Nan, *J. Materiomics*, 2 (2016) 265.
14. 14.Y.K. Sun, S.W. Oh, C.S. Yoon, H.J. Bang and J. Prakash, *J. Power Sources*, 161 (2006) 19.
15. T.A. Arunkumar and A. Manthiram, *Electrochem. Solid-State Lett.*, 8 (2005) A403.
16. Z. Yang, Y. Jiang, J.H. Kim, Y. Wu, G.L. Li and Y.H. Huang, *Electrochim. Acta*, 117 (2014) 76-83.
17. H.Y. Sun, X. Kong, B.S. Wang, T.B. Luo and G.Y. Liu, *Int. J. Electrochem. Sci*.,12 (2017) 8609.
18. R.L. David, *CRC handbook of chemistry and physics*, National Institute of Standards and

Technology, (2003) New York, the United States.
19. G.B. Zhong, Y.Y. Wang, X.J. Zhao, Q.S. Wang, Y. Yu and C.H. Chen, *J. Power Sources, 2*16 (2012) 368.
20. L.P Wang, H. Li, X.J. Huang and E. Baudrin, *Solid State Ionics*, 193 (2011) 32.
21. J. Liu and A. Manthiram, *J. Phys. Chem. C,* 113 (2009) 15073.
22. S. Patoux, L. Daniel, C. Bourbon, H. Lignier, C. Pagano, F.C. Le, S. Jouanneau and S. Martinet, *J. Power Sources,* 189 (2009) 344.
23. J.H. Kim, S.T. Myung, C.S. Yoon, S.G. Kang and Y.K. Sun, *Chem. Mater.,* 16 (2004) 906.
24. J.M. Zheng, J. Xiao, X.Q. Yu, L. Kovarik, M. Gu, F. Omenya, X.L. Chen, X.Q. Yang, J. Liu, G.L. Graff, M.S. Whittingham and J.G. Zhang, *Phys. Chem. Chem. Phys.,* 14 (2012) 13515.
25. J. Guo, Y.J. Li, Y.X. Chen, S.Y. Deng, J. Zhu, S.L. Wang, J.P. Zhang, S.H. Chang, D.W. Zhang, X.M. Xi, *J. Alloy. Compd.*, in press. https://doi.org/10.1016/j.jallcom.2019.152031.
26. Q. Chang, A.J. Wei, W. Li, X. Bai, L.H. Zhang, R. He and Z.F. Liu, *Ceram. Int*., 45 (2019) 5100.
27. Q. Wu, K. Xue, X.H. Zhang, X.S. Xie, H.Q. Wang, J.J. Zhang and Q.Y. Li, *Ceram. Int.*, 45 (2019) 5072.
28. X.H. Rui, N. Ding, J. Liu, C. Li and C.H. Chen, *Electrochim. Acta*, 55 (2010) 2384.